SLAC – PUB – 3817
October 1985
(T/E)

Search for Anomalous Single Photon Production at PEP*

G. Bartha, D. L. Burke, P. Extermann,[a] P. Garbincius,[b]
C. A. Hawkins, R. J. Hollebeek, M. J. Jonker, L. Keller,
C. Matteuzzi,[c] N. A. Roe, T. R. Steele, and R. J. Wilson

Stanford Linear Accelerator Center
Stanford, California 94305
and

A. S. Johnson and J. S. Whitaker[d]

Massachusetts Institute of Technology
Cambridge, Massachusetts 02139
and

C. Hearty, J. E. Rothberg, and K. K. Young

University of Washington
Seattle, Washington 98195

(Submitted to *Physical Review Letters*)

This Letter reports a search for the production by e^+e^- annihilation of a single photon accompanied by particles that interact only weakly in matter. The search was performed at PEP ($\sqrt{s}$ = 29 GeV) with a new detector, ASP. No unexpected signal was observed. The limit $N_\nu < 14$ (90% CL) is placed on the number of light neutrino species, and the mass of scalar electrons predicted by theories of supersymmetry is constrained to $m_{\tilde{e}} > 51$ GeV/c^2 (90% CL) for $m_{\tilde{\gamma}} = 0$ and degenerate $\tilde{e}$ mass states.

⋆ This work was supported in part by the Department of Energy, contract DE-AC03-76SF00515 (SLAC), and by National Science Foundation Grant PHY-8503215.

a Permanent address: University of Geneva, Geneva, Switzerland
b Permanent address: Fermi National Laboratory, Batavia, Illinois 60510, U. S. A.
c Present address: CERN, EP Division, CH-1211 Geneva 23, Switzerland
d Present address: Boston University, Boston, Massachusetts 02215, U. S. A.

This Letter reports the results of a search for the production by e^+e^- annihilation of new particles that interact only weakly in matter and therefore are not directly observable. This is done by searching for production of these new particles accompanied by the radiation of a single photon,

$$e^+e^- \to \gamma + \text{weakly interacting particles.} \qquad (1)$$

The radiative production of neutrino pairs by the standard weak charged and neutral currents contributes to (1)[1]. At $\sqrt{s} << m_W$,

$$\frac{d\sigma(e^+e^- \to \gamma\nu\bar{\nu})}{dE_\gamma d\cos\theta_\gamma} \sim \frac{\alpha^3}{\sin^4\theta_W} \cdot \frac{(1+N_\nu/4)}{p_T^\gamma \cdot \sin\theta_\gamma} \cdot \frac{s}{m_W^4} \quad , \qquad (2)$$

where N_ν is the number of light neutrino species, and p_T^γ and θ_γ are the momentum transverse to the beam axis and the polar angle of the radiated photon. For $N_\nu = 3$ the exact cross section[2] corresponds to 1.0 observed event in the acceptance of the search reported in this Letter.

Theories of supersymmetry (SUSY) predict the existence of particles that also contribute to (1)[3,4]. Many SUSY models contain a photino $\tilde{\gamma}$ that is stable, interacts weakly in matter, and is produced in pairs by the exchange of a scalar electron $\tilde{e}$. At $\sqrt{s} << m_{\tilde{e}}$,

$$\frac{d\sigma(e^+e^- \to \gamma\tilde{\gamma}\tilde{\gamma})}{dE_\gamma d\cos\theta_\gamma} \sim \alpha^3 \cdot \frac{1}{p_T^\gamma \cdot \sin\theta_\gamma} \cdot \frac{s}{m_{\tilde{e}}^4} \quad . \qquad (3)$$

There are, in general, two $\tilde{e}$ mass eigenstates that contribute to the $\gamma\tilde{\gamma}\tilde{\gamma}$ final state. If these are degenerate, the effective cross section will be twice that for the case in which one mass is much larger than the other. SUSY also predicts the existence of scalar neutrinos $\tilde{\nu}$ which can be produced through the normal weak neutral current and through supersymmetric charged currents.[4]

From (2) and (3) it is clear that good photon detection efficiency down to small values of p_T^γ and θ_γ is desirable. Isolation of process (1) from backgrounds requires nearly complete solid angle coverage with electromagnetic calorimetry and charged particle tracking. The most difficult background to eliminate comes from the process $e^+e^- \to e^+e^-\gamma$. The kinematics of this process require complete veto capability at $\theta > \theta_{veto} = p^\gamma_{Tmin}/2E_{beam}$. The acceptance of the experiment reported in this Letter is $p^\gamma_{Tmin} > 1$ GeV with $E_{beam} = 14.5$ GeV, i.e. $\theta_{veto} = 34$ mr. The ASP detector described below has no gaps above $\theta = 21$ mr.

The ASP detector is shown in Fig. 1. Photons produced at central polar angles are detected in five-layer stacks of lead-glass bars interleaved with proportional wire chambers (PWCs). These stacks completely surround the interaction point (I. P.) in azimuth. The glass bars are 6 cm × 6 cm × 75 cm, and each is read out by a single phototube. The bars are staggered along the beam direction Z (Fig. 1b) to eliminate cracks and provide optimal resolution of the origin of electromagnetic showers. The energy resolution of the calorimeter is measured with radiative Bhabha events (see below) to be 15% at 1 GeV when averaged over all angles with $\theta > 20°$. The PWCs are made from 1.2 cm × 2.4 cm closed-cell aluminum extrusions and provide position information in the plane perpendicular to the beam.

Charged particles are tracked between the beam pipe and central calorimeter by planes of proportional tubes with resistive sense wires parallel to the beam line. These wires are read out on both ends to provide redundancy and, by charge division, the Z coordinate of charged tracks. The central tracker is surrounded by 2 cm thick veto scintillators with phototubes on both ends. The pair conversion probability of a photon in the material between the I. P. and the veto scintillators

is 4.5% at $\theta_\gamma = 90°$.

Calorimeter modules made from lead and scintillator surround the beam pipe in the forward angle region (Fig. 1b). Proportional tubes measure the spatial positions of showers at a depth of 6 X_0 in these modules. The forward calorimeter modules overlap each other and the central calorimeter so that no gaps occur in the detector above $\theta = 21$ mr. Four drift chamber planes track charged particles at polar angles between 21 and 100 mr.

The detector is located 20 m underground. This filters all primary hadrons from the cosmic ray flux and reduces the overall intensity by a factor of ≈ 2.7. Scintillation counters above the detector provide an additional order of magnitude rejection of cosmic rays.

Signals from the lead-glass bars are electronically summed and discriminated to generate hardware triggers. The detector is triggered at a threshold of 1.5 GeV on the total pulse height from all phototubes. It is also triggered above 0.6 GeV by requiring that the lead-glass signal be localized to a single quadrant, or adjacent quadrants, and that it be seen in more than one layer. Signals from the forward shower modules are used to trigger on small angle Bhabha scattered electrons. A special trigger for radiative Bhabha ($ee\gamma$) events is formed by placing the small-angle Bhabha trigger in coincidence with a very low (≈ 0.2 GeV) threshold on the total lead-glass pulse height.

The $ee\gamma$ triggers are kinematically fitted off-line using the forward calorimeters and the charged particle tracking (but not the lead glass) to produce a sample (45,000 events) of electrons and photons with known energies and production angles. This sample is used to study the performance of the central calorimeter. The efficiency of the trigger is measured to be $> 99\%$ for single photons produced

at the I. P. with $p_T^\gamma \geq 1$ GeV and $\theta_\gamma > 20°$. This is taken to be the fiducial region for our signal.

Photon candidates are selected off-line by requiring a cluster of blocks in the central calorimeter with a pattern consistent with an electromagnetic shower. The time of the lead-glass pulse is required to be within $\pm\ 3\,\sigma_T$ of the known beam crossing time; $\sigma_T = 2.4$ ns at 1 GeV and slightly less at higher energies. The candidate photon is fitted to extract R, the signed projected distance of closest approach to the known I. P. in the XZ or YZ plane. The photon candidate is kept if there is a good fit with $|R| < 30$ cm; $\sigma_R = 3$ cm. (See Fig. 3.) The efficiency of all photon selection criteria is measured as a function of photon energy and angles with the fitted $ee\gamma$ and $e^+e^- \rightarrow \gamma\gamma$ events. The average photon detection efficiency is measured to be 75% in the signal region, with little variation in E_γ and θ_γ. The majority of the reconstruction losses occur at azimuths where showers span two lead glass quadrants.

The ability to isolate the single-photon final state from background depends upon electronic noise levels and occupancies in the components of the detector. Triggers taken on randomly chosen beam crossings are used to determine these levels. Radiative Bhabha and $e^+e^- \rightarrow \gamma\gamma$ events are used to study occupancies that are correlated with the presence of the signal photon, such as backsplash into the veto scintillators and central tracker, and leakage into the forward shower modules. Cuts against backgrounds are determined for each element of the detector; no single cut results in more than a 10% loss of signal efficiency.

The candidate signal events are taken to be those with a single good photon candidate at $\theta_\gamma > 20°$ and no significant signal seen anywhere else in the detector. Three events with single photons with energies consistent with the beam energy

were observed in the data sample. These are interpreted as $e^+e^- \rightarrow \gamma\gamma$ events in which one of the photons escapes the detector without showering. A study of the observed $e^+e^- \rightarrow \gamma\gamma$ data sample predicts 1.5 single photons from this source. The requirement $E_\gamma < 12$ GeV, determined from an analysis of Bhabha events, eliminates this background with negligible loss of signal acceptance. The resulting sample of events with $p_T^\gamma > 0.5$ GeV is displayed in Fig. 2. There are two events with $p_T^\gamma > 1.0$ GeV/c. With the measured efficiencies for the photon reconstruction and isolation cuts, the overall efficiency for photons produced in our signal region is 45%. This includes losses due to photon conversion in the beam pipe and central tracker and the effects of finite resolutions in photon energy and angle.

Signal and background events have different R distributions. The R distribution of signal photons is measured with the $ee\gamma$ sample and is shown in Fig. 3a. The background at low p_T^γ (Fig. 2) is mainly due to interactions between beam particles and residual gas in the beampipe. This background is observed to be flat in R before application of several of the photon pattern cuts that are biased to accept showers with small R. The shape of the final background is measured by relaxing cuts other than these pattern cuts, and is shown in Fig. 3b.

With the measured distributions (Fig. 3) for signal, $P_S(R)$, and background, $P_B(R)$, we maximize the log-likelihood function,

$$ln\left(\frac{e^{-(S+B)} \cdot (S+B)^{N_{ev}}}{N_{ev}!}\right) + \sum_{i=1}^{N_{ev}} ln\left(\frac{S \cdot P_S(R_i) + B \cdot P_B(R_i)}{S+B}\right) \qquad (4)$$

to obtain the best estimate from the experimental data of the number of signal events S and background events B. For a given true number of signal and

background events, the confidence level of this experiment is computed by Monte Carlo as the fraction of equivalent experiments that would estimate a number of signal events larger than S. We find that for 2.9 true signal events the confidence level is 90% for the two events that we observe. The 95% CL is given by 3.9 true signal events.

The integrated luminosity is measured with tracked small-angle Bhabha events to be 68.7 pb^{-1}. With the previously discussed efficiency we obtain the 90% CL limit,

$$\sigma(e^+e^- \to \gamma + \text{weakly interacting particles}) < 0.094 \text{ pb} \qquad (5)$$

for $E_\gamma < 12$ GeV, $p_T^\gamma > 1.0$ GeV/c and $\theta_\gamma > 20°$. Since the detection efficiency is nearly constant with E_γ and θ_γ in the signal region, the limit (5) does not depend greatly on the produced photon spectrum or angular distribution. The cross section for radiative pair production of three neutrino species is[2] 0.032 pb with photons in our fiducial region, so (5) places the limit 0.062 pb on any possible anomalous contribution to (1).

From (5) we deduce the limit $N_\nu < 14$ (90% CL) on the total number of light neutrino species. The 95% CL limit is $N_\nu < 20$. The validity of these limits requires no assumptions other than the standard coupling of the Z^0 to neutrinos. From the exact cross section[5] for $e^+e^- \to \gamma\tilde{\gamma}\tilde{\gamma}$ we deduce the limits shown in Fig. 4 on the $\tilde{e}$ and $\tilde{\gamma}$ masses. From the model of reference 4 for $\tilde{\nu}$ production, we obtain the limit $m_{\widetilde{W}} > 48$ GeV/c^2 (90% CL) using the parameter values $m_{\tilde{\nu}} = 0$, $O^+ = 1$, and $m_1 << m_2$. These limits are significantly larger than those given by previously published searches[6] and, for $m_{\tilde{\gamma}} = 0$, our limit $m_{\tilde{e}} > 51$ GeV/c^2 already rules out the decay of real Z^0s to degenerate $\tilde{e}$ pairs.

We thank D.Chambers, R.Baggs, D.Forbush, T.Lyons, C.Noyer, K.Skarpass, and R.Stickley for considerable technical assistance with the construction and installation of the detector. We are also grateful to the PEP operations staff. One of us (JSW) acknowledges support under the Department of Energy Outstanding Junior Investigator program.

References

1. E. Ma and J. Okada, Phys. Rev. Lett. 41, 287 (1978).
2. K. J. F. Gaemers, R. Gastmans, and F. M. Renard, Phys. Rev. D19, 1605 (1979).
3. J. A. Grifols, X. Mor-Mur, and J. Solá, Phys. Lett. 114B, 35 (1982); P. Fayet, Phys. Lett. 117B, 460 (1982); J. Ellis and J. S. Hagelin, Phys. Lett. 122B, 303 (1983).
4. J. S. Hagelin, G. L. Kane, and S. Raby, Nucl. Phys. B241, 638 (1984).
5. K. Grassie and P. N. Pandita, Phys. Rev. D30, 22 (1984).
6. A. J. Behrends *et al.*, (CELLO Collaboration), Phys. Lett. 114B, 287 (1982); L. Gladney *et al.*, (Mark II Collaboration), Phys. Rev. Lett. 51, 2253 (1983); W. Bartel *et al.*, (JADE Collaboration), Phys. Lett. 152B, 385 (1985); E. Fernandez *et al.*, (MAC Collaboration), Phys. Rev. Lett. 54, 1118 (1985).

Figure Captions

Figure 1. (a) Cross sectional view of the ASP central calorimeter and tracking system. Only a section of the central tracker is shown; it completely surrounds the I. P.

(b) Side view of one quarter of the ASP detector. Only the horizontal lead glass bars are shown in this view; there are 632 bars in the detector.

Figure 2. Final sample of single photon candidates with $p_T^\gamma > 0.5$ GeV/c and $\theta_\gamma > 20°$.

Figure 3. (a) R-distribution of radiative photons in the signal region. The line is Gaussian with $\sigma = 3$ cm at $|R| < 6$ cm and exponential at $|R| > 6$ cm.

(b) R-distribution of background events with $p_T^\gamma > 0.6$ GeV/c described in the text. The line is a Gaussian with $\sigma = 12$ cm.

Figure 4. Limits (90% CL) placed on $\tilde{e}$ and $\tilde{\gamma}$ masses by this experiment. The solid line is the limit for degenerate $\tilde{e}$ masses, and the dashed-dot line is the limit if only one mass eigenstate contributes to the cross section. The 95% CL is $m_{\tilde{e}} > 44$ GeV/c^2 for degenerate mass states and $m_{\tilde{\gamma}} = 0$.

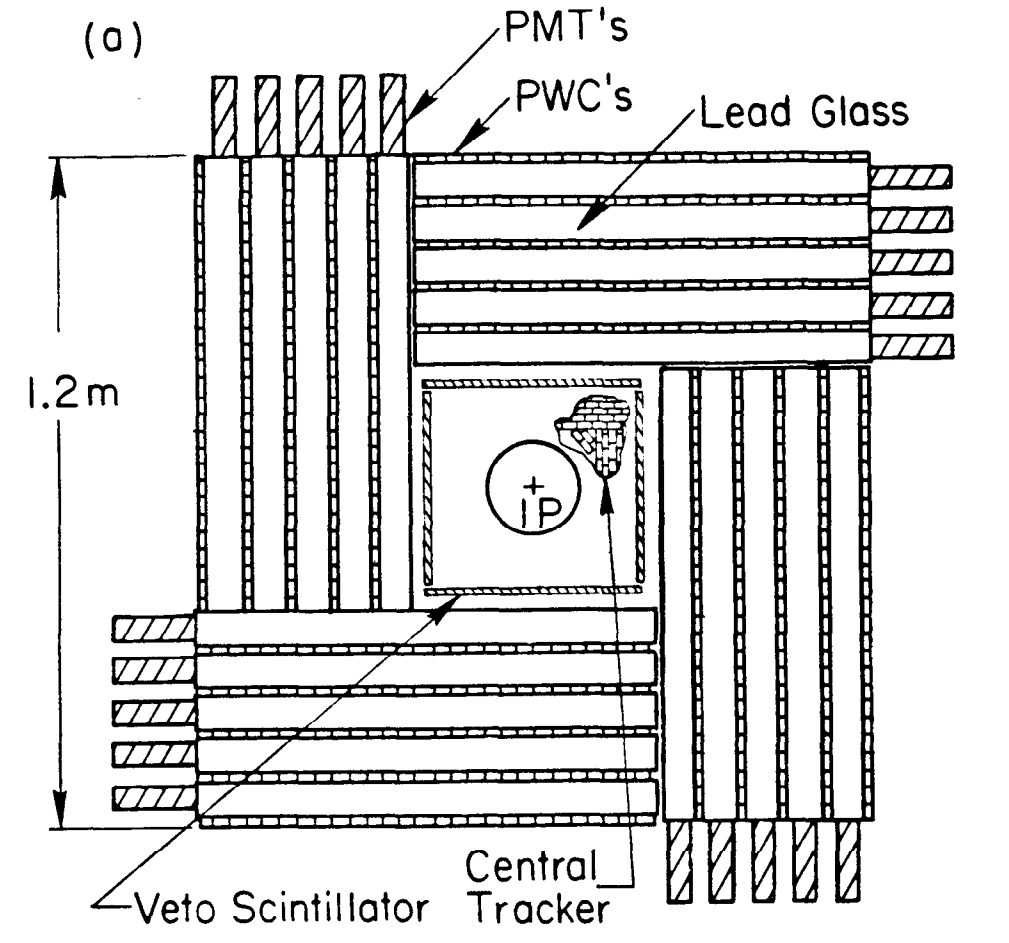
(a)
PMT's
PWC's
Lead Glass
1.2m
IP
Veto Scintillator
Central Tracker

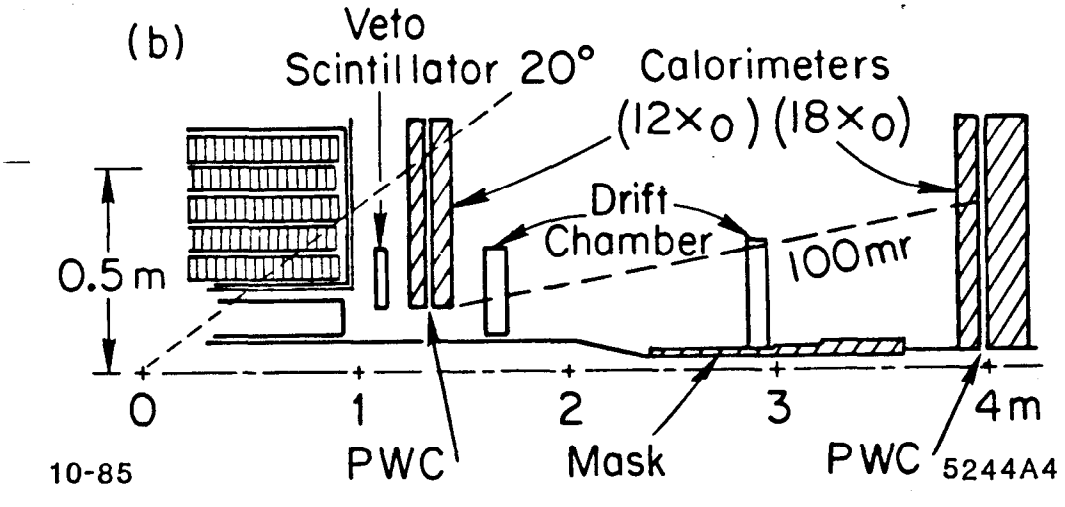
(b)
Veto Scintillator
20°
Calorimeters
(12×o) (18×o)
Drift Chamber
100mr
0.5 m
0
1
2
3
4m
PWC
Mask
PWC
10-85
5244A4

Fig. 1

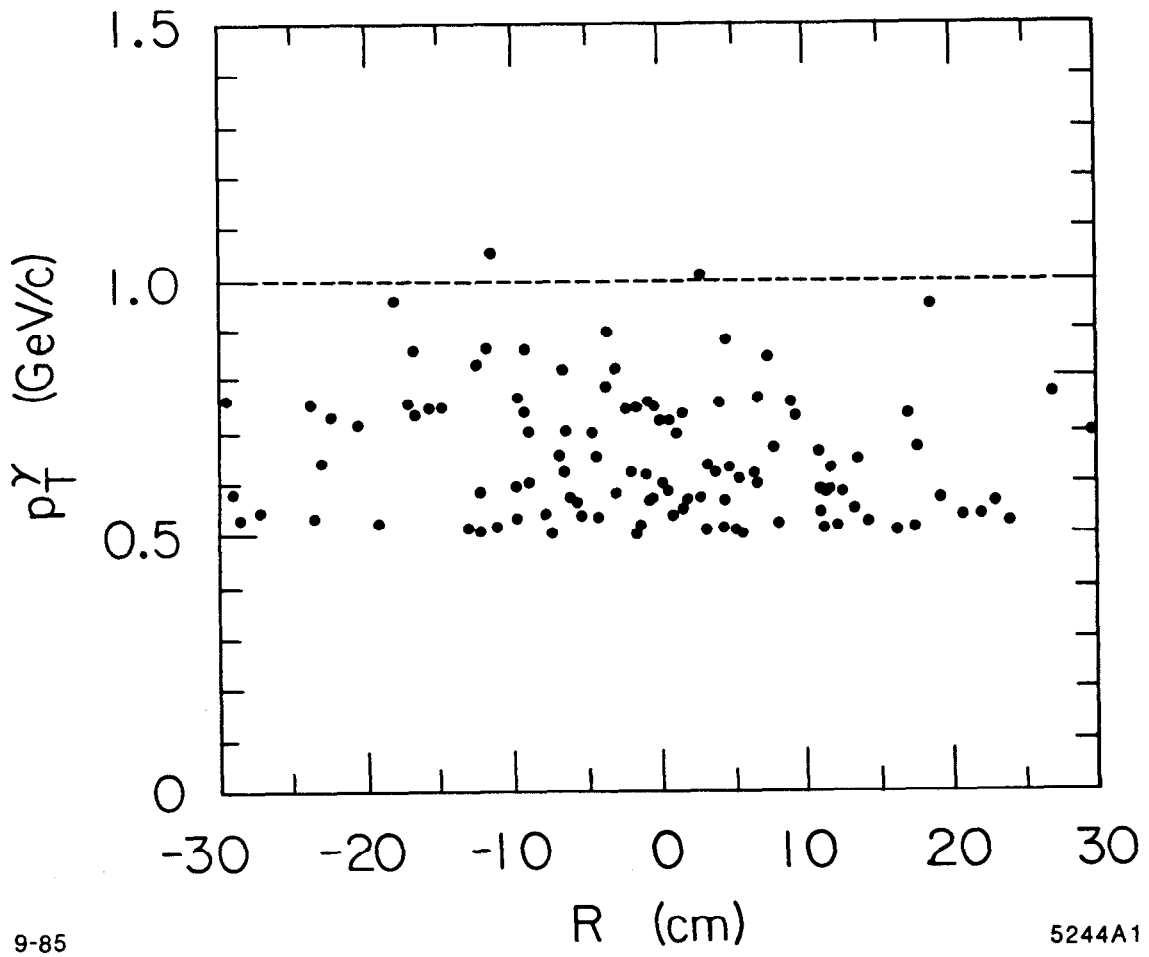

Fig. 2

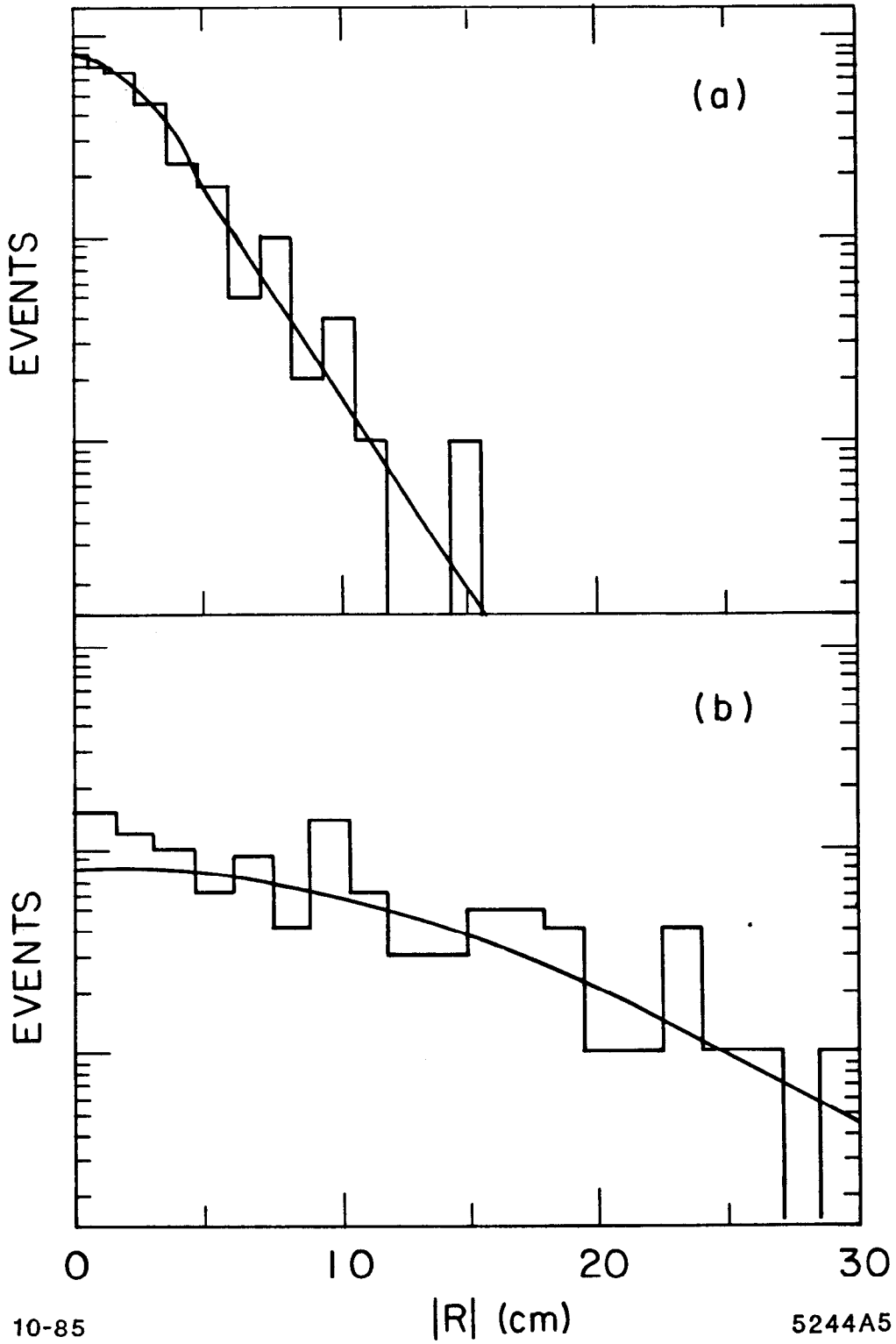

Fig. 3

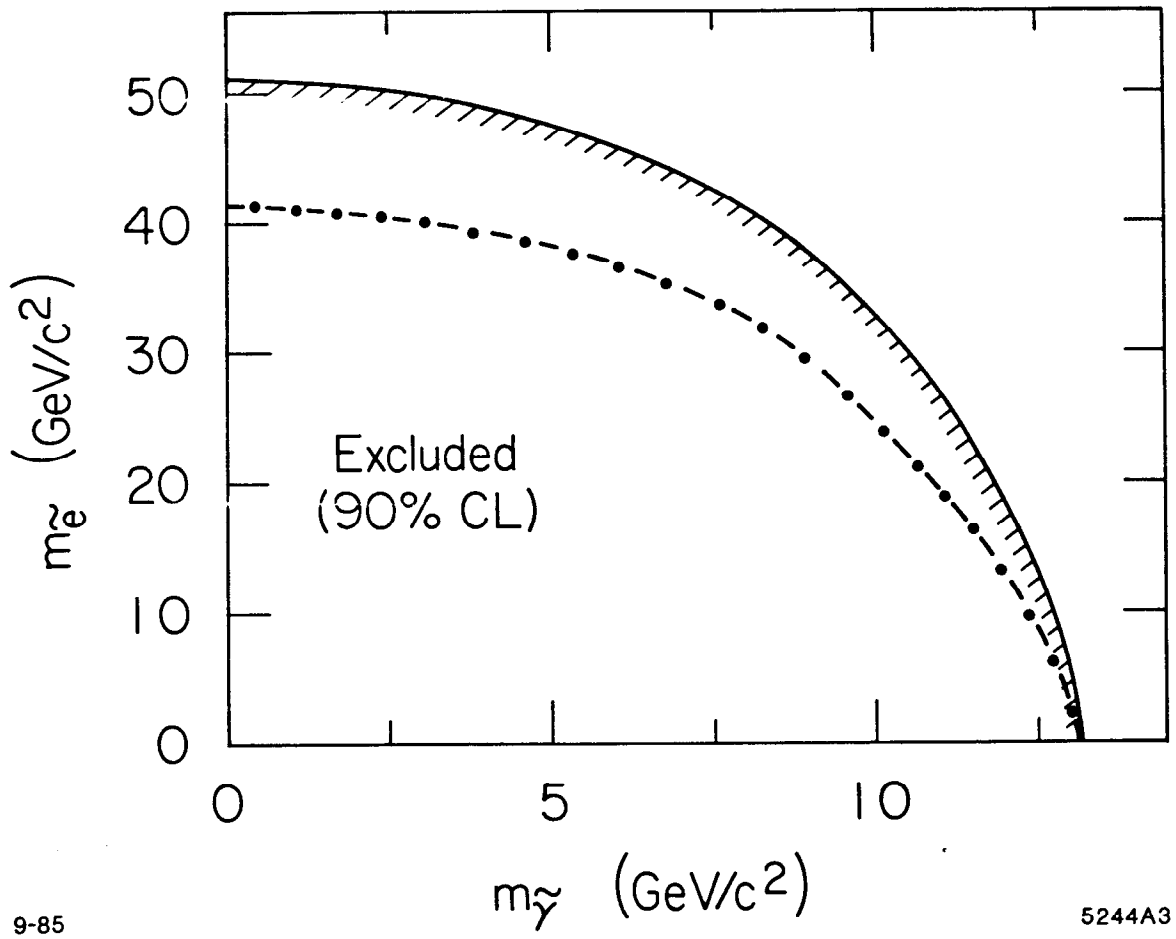
50
40
30
20
10
0
0
5
10
Excluded
(90% CL)
$m_{\tilde{e}}$ (GeV/c^2)
$m_{\tilde{\gamma}}$ (GeV/c^2)
9-85
5244A3

Fig. 4